Chapter 6

The Collapse

A nest has been constructed and methods leading to conception have been tried out. The next event is that, from out of a turbulent cloud, the eggs are somehow laid: dense and bound cores form in regions where the turbulence has partly abated.

In this chapter, we deal with the ensuing pregnancy. In the classical problem, we wish to determine what core 'initial conditions' lead to young stars i.e. the properties which determine the fertility of the embedded eggs. In this approach, we aim to extract the physical laws which control the masses of stars. These laws are fundamental to the nature of our Universe and our existence. We now examine and analyse cores without anticipating the outcome. The constraints we could impose from the known adult star populations – the statistics of main-sequence star populations – will only be applied when the story is more developed (in §11.9).

This chapter then brings us to the final preparations: the internal adjustments before the moment of birth. The inexorable collapse may then begin.

6.1 Observing Starless Cores and Pre-stellar Cores

Starless cores are dense cores in which no protostars or stars of any kind are embedded. Yet, many cores were found to already contain embedded objects when in 1983 the Infrared Astronomy Satellite surveyed the sky in the far-infrared spectral range 12–100 μm. The time scales and statistics provide evidence that both types of cores are transient with lifetimes of order of 1 Myr.

We define the subset of cores which are fertile as pre-stellar cores. These are the eggs in which a protostar is destined to be nurtured. On the other

hand, the acronym EGG stands for Evaporating Gaseous Globule. This defines another subset of cores in which nearby massive stars are having a strong influence on egg formation and development. The influence is effected by UV heating which evaporates the outer layers and pressurises the inner layers.

Starless cores are larger in size and tend to be less centrally condensed than those already with embedded sources. They also typically contain sufficient mass to form a protostar and it's envelope. Hence they are clearly *the* potential birth sites. However, although they could be on the verge of gravitational collapse, they may equally be unbound structures about to disperse. Hence, a starless core is also a pre-stellar core if the collapse can no longer be aborted and star birth is inevitable. We can probably pick out the pre-stellar cores from them as those displaying indications of infall and/or exhibiting a central density peak.

We have only recently had the technology to describe starless cores and, obviously, the first issue we want to settle is whether they are collapsing or not. Two techniques are used: isotopic molecular line emission and dust continuum emission. Certain molecular lines such as from NH_3, CS and HCO^+, provide some evidence for inward gas motions through Doppler spectroscopy. The spectral signatures of mass infall suggest that the proto-stellar collapse has already started in some cores but these signatures only become obvious after the birth (§7.8).

The cores are very cold and so emit most of their light at submillimetre and millimetre wavelengths. At low temperatures, the continuum radiation is generated by dust particles. The dust emission is generally optically thin at these wavelengths which has the advantage that the mission is directly proportional to the total mass involved, although several factors (as always) such as the relative amounts of dust and gas (the dust-to-gas ratio) and non-uniformity may well complicate the calculation. A single dust grain emits and absorbs radiation as a blackbody proportional to an effective surface area and the well-known Planck function

$$B(\nu) = \frac{2\,h\,\nu^3}{c^2}\frac{1}{\exp(\frac{h\nu}{kT_d} - 1)} \tag{6.1}$$

where T_d is the dust temperature, h is the Planck constant and c is the speed of light. Note that the flux density B has CGS units of $\mathrm{erg\,s^{-1}\,cm^{-2}\,Hz^{-1}}$ but is usually expressed in Janskys where $1\,\mathrm{Jy} = 10^{-26}$ of the CGS value. Even so, the fluxes we detect tend to be some small fraction of a Jansky.

The blackbody curve possesses a maximum at

$$\nu_{max} = 58.8 T_d \text{ GHz}, \quad \text{or} \quad \lambda_{max} = \frac{0.510}{T_d} \text{ cm}, \tag{6.2}$$

which only depends on the temperature (Wien's Law). Thus, the continuum emission from a cold molecular cloud of temperature 10 K peaks at 600 GHz or 0.5 mm, in the submillimetre regime.

Other expressions are found in the literature. For example, astronomers often prefer to plot $\nu \cdot S(\nu)$ instead of the observed flux $S(\nu)$ since this is an energy flux, and so demonstrates the spectral region containing most of the power emitted rather than where most of the photons are detected. An analogous spectral energy in terms of wavelength is often employed, $\lambda \cdot S(\lambda)$, where $S(\lambda)$ is the flux per unit wavelength.

The predicted maxima of these quantities are

$$\nu_{max} = 81.7 \; T_d \text{ GHz} \quad \textit{or} \quad \lambda_{max} = \frac{0.367}{T_d} \text{ cm} \tag{6.3}$$

for blackbodies. The majority of astronomers express the *spectral energy distribution* (SED) in terms of wavelength. However, if the flux density is in Janskys, then the first expression will still apply.

Integration over the entire spectrum of a blackbody yields a luminosity which depends only on the temperature,

$$I_{bb} = \frac{\sigma_{bb}}{\pi} T_d^4, \tag{6.4}$$

where $\sigma_{bb} = 5.670 \times 10^{-5}$ erg s^{-1} cm^{-2} K^{-4} is the Stefan-Boltzmann constant.

Unfortunately, trying to fit a pristine blackbody curve to yield the temperature, luminosity, and hence the mass, often fails. Observations of cores now extend over several wavebands, in some of which the core is optically thick. The radiation is then modelled with a modified blackbody spectrum. This modified spectrum is often called a greybody curve and is calculated according to the rule

$$I(\nu) = B(\nu)(1 - e^{-\tau_\nu}), \tag{6.5}$$

where the optical depth through the intervening dust τ is quite a complex function of frequency.

We often assume a power-law representation, $\tau_\nu = (\nu/\nu_0)^{\beta_o}$, for the optical thickness at frequency ν with ν_0 being selected such that $\tau_\nu = 1.0$ at $\nu = \nu_0$. The optical depth will be proportional to the column of gas, $N(H)$,

and the dust absorption cross section, σ_λ. The wavelength dependence is quite complex, with one useful approximation being given by

$$\sigma_\lambda = b\frac{\tau}{N(H)} = 7 \times 10^{-25}\left(\frac{\lambda}{100\mu m}\right)^{\beta_o} \text{ cm}^2, \tag{6.6}$$

where $b = 1$ and $\beta_o = -1.5$ for $40\mu m < \lambda < 100\mu m$ and $\beta_o = -2$ for $\lambda > 100\mu m$.

The dust opacity κ is commonly used in the optically thin limit $I(\nu) = \tau_\nu B(\nu)$ where $\kappa = \sigma_\lambda / m_H$ (note that dust opacity and emissivity are equivalent according to Kirchoff's law). The opacity increases as the gas particles stick onto the dust grains. For example, $\kappa \sim 0.005\,\text{cm}^2\,\text{gm}^{-1}$ at 1.3 mm in clouds, but it is typically a factor of 2 larger in dense locations such as cores and probably 4 times larger in the disks which may go on to form planets (protoplanetary disks, see §9.4.2).

In practice, β_o is available as a parameter to be determined by a fitting procedure. It embraces information about the dust type and evolution. For example, a very steep function with $\beta_o = 2.8$ was found for a massive giant molecular cloud core GCM 0.25+0.11 located near the Galactic centre. The high exponent is consistent with the presence of dust grains covered with thick mantles of ice. For the starless core L 1544, Figure 6.1 shows again that β_o is quite high in comparison to a protostellar core. For the same reason, molecular lines are unreliable as tracers of gas density in dense cores since molecules may freeze out in large quantities, forming ice mantles around refractory grain particles.

In the light of these complications, it makes sense to characterise a core by a bolometric luminosity and temperature. The bolometric luminosity is simply the total luminosity summed over the entire spectrum and the bolometric temperature is defined as the temperature of a blackbody whose spectrum has the same mean frequency $< \mu >$ as the observed spectrum. We find

$$T_{bol} = 1.25\frac{< \nu >}{100 \text{ GHz}} \text{ K}. \tag{6.7}$$

Therefore, as a core gets hotter, the mean frequency shifts upwards.

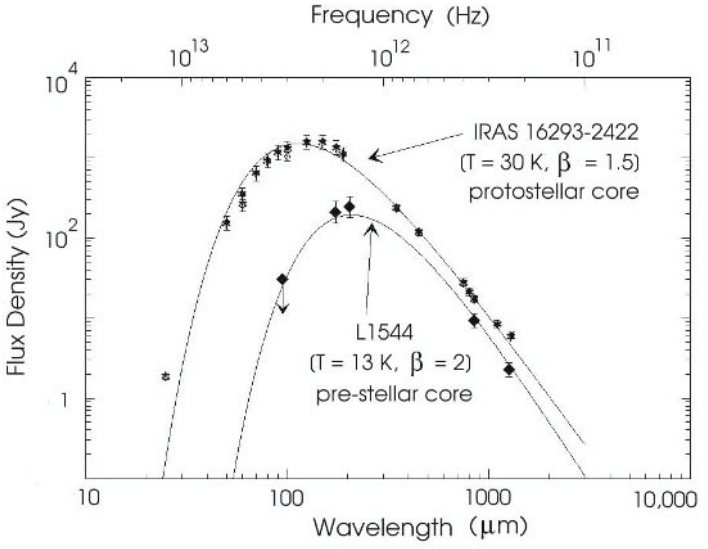

Fig. 6.1 The spectrum of the starless core L 1544 and the protostellar core IRAS 16293-2422, fitted with greybody curves. (Credit: from data presented by P. André, D. Ward-Thompson & M. Barsony in Protostars and Planets IV, edited by V. Mannings, A. P. Boss & S. S. Russell, 2000 (University of Arizona Press).)

6.2 Properties of Starless Cores

6.2.1 *Physical parameters*

Most observed cores contain sufficient mass to form stars. Derived masses range from $0.05\,M_\odot$ to $30\,M_\odot$. The smallest detected cores might go on to form brown dwarfs rather than stars since the critical mass required in order to be able to commence hydrogen burning (fusion) is $\sim 0.075\,M_\odot$ (§12.1).

Temperatures are typically under 15 K. This means that the dust is cold, consistent with the absence of a warming embedded protostar. For example, a temperature of 13 K is determined for the L 1544 starless core in Taurus. A model fit is shown in Fig. 6.1. A confident result requires data from a wide spectral region – data in this figure were acquired from several telescopes: the Infrared Space Observatory ISO, James Clerk Maxwell Telescope (JCMT, Hawaii) and the Institut de Radioastronomie Millimetrique

(IRAM, Spain), thus combining innovative technology from many nations.

Can the cores be thermally supported? Observed line widths are narrow, typically under 0.5 $\mathrm{km\,s^{-1}}$ with a mean value of 0.3 $\mathrm{km\,s^{-1}}$. The mean value implies one-dimensional velocity dispersions of 0.13 $\mathrm{km\,s^{-1}}$. Heavy molecules, however, possess very small line widths in a thermal gas. The lines being measured are associated with heavy molecules such as N_2H^+ (29 atomic mass units), which are slow moving in a thermal gas. Therefore, the expected velocity dispersion due to thermal motions alone is extremely small, about 0.05 $\mathrm{km\,s^{-1}}$ for a temperature of 10 K. The motions of *these molecules* are predominantly due to turbulence. The motions are, however, not supersonic but mildly subsonic, given the sound speed of 0.19 $\mathrm{km\,s^{-1}}$ from Eq. 3.9. Therefore, thermal pressure dominates but turbulence still makes a sizable contribution.

The structure of a pre-stellar core is exemplified by the L 1544 core. It consists of a dense kernel surrounded by a low density envelope (Fig. 6.2). From dust emission and absorption observations, we know that the kernel has a central density of about $10^6\,\mathrm{cm^{-3}}$ inside a radius $R_{\mathrm{flat}} = 2,500\,\mathrm{AU}$ (an elongated region). This is followed by a $1/\mathrm{R}^2$ density fall-off until a radius of about 10,000 AU. This 'central flattening' is quite common, with a break to a steeper fall-off occurring at about 6,000 AU (0.03 pc). Typically, cores are not round or elliptical but roughly elongated with aspect ratios in the range 2–3. They may well be prolate or triaxial rather than oblate. Some even appear completely irregular. Hence, to describe the density distribution, a core centre is first defined as the centroid of the dust emission and the radial density distribution is then an angle-averaged quantity.

6.2.2 *Dynamical parameters*

Inward motions are inferred by observing the *infall asymmetry* in spectral lines. A necessary signature is a combination of a double peak with a brighter blue component or a skewed single blue peak in an optically thick emission line. We need to discard the possibility that two unrelated clouds are superimposed and their combined signature imitates a collapse signature. This can be achieved by checking for a simple Gaussian single peak in an optically thin line. In addition, other systematic motion – rotation and outflow – must be distinguished.

As we gather data, a picture of how starless cores evolve is emerging. Cores occasionally show evidence for infall with very low speeds in the range of 0.05–0.09 km $\mathrm{s^{-1}}$. L1544 can be regarded as an archetypal pre-stellar

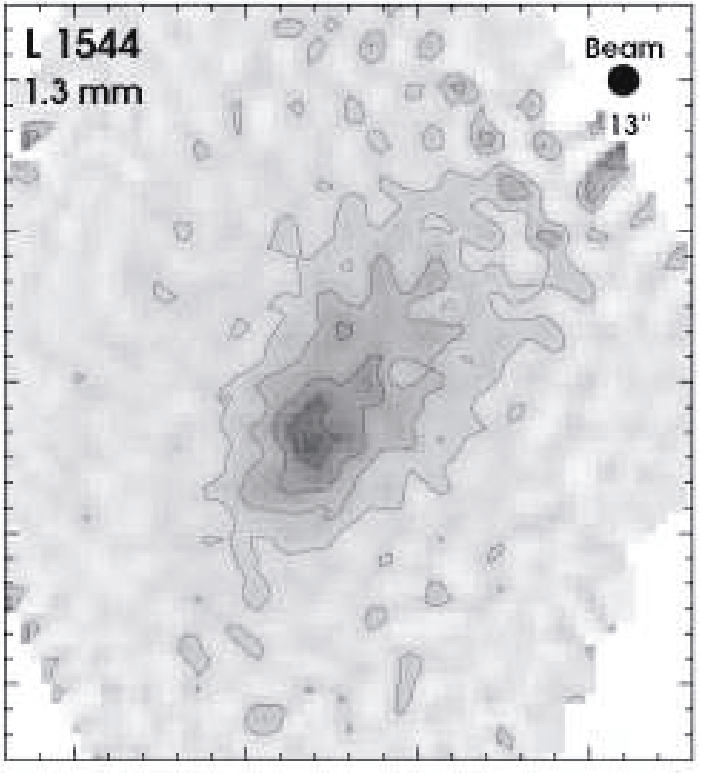

Fig. 6.2 The starless core L 1544 at 1.3 mm. (Adapted from paper by D. Ward-Thompson, F. Motte & P. André, MNRAS 305, 143–150.)

core: a starless core which is entering the stage of rapid infall. We find that the infall typically extends to radii of 0.06–0.14 pc. This extended infall phenomenon may be a necessary stage in core evolution.

The chemical composition is systematically differentiated. Near the core centres, some molecules, including CO and CS, almost vanish. In contrast, NH_3 increases toward the core centre while the N_2H^+ molecule maintains a constant abundance. These observations are consistent with a model in which CO is able to condense onto dust grains at densities above $10^5\,\mathrm{cm}^{-3}$. The corresponding radius of the inner depleted region is typically $R_d \sim$ 6,500 AU.

The angular momentum of cores can be evaluated through molecular

tracers such as NH_3. Cores in the size range 0.06–0.6 pc are observed to rotate in the majority of cases studied with velocity gradients in the range 0.3–3 km s^{-1} pc^{-1} (corresponding to 10^{-14}–10^{-13} s^{-1}). Here, the angular velocity Ω scales roughly as $R^{-0.4}$ and the specific angular momentum J/M scales roughly as $R^{1.6}$, with a value of 10^{21} cm^2 s^{-1} on the smallest scales measured. The ratio of rotational kinetic energy to the absolute value of the gravitational energy shows no trend with R and has a mean value of about 0.03 with a large scatter. It is also found that cores tend to have gradients that are not in the same direction as gradients found on larger scales in the immediate surroundings, an effect which again suggests the presence of turbulence.

We could constrain our theories if we knew how long starless cores survive. The dynamical time scale of those exhibiting infall is $0.1\,\mathrm{pc}/0.1\,\mathrm{km\,s^{-1}}$ $\sim 10^6\,\mathrm{yr}$. So this should be a strict minimum (at least for the cores which are present long enough to favour detection). The ratio of the number of starless cores to the number of cores with very young protostars is about 3, suggesting that the typical lifetime of starless cores is 0.3–1.6 Myr (3 times longer than the estimated duration of the Class 0 and Class I phases, §7.8).

The above facts do more than constrain the theory: most models developed in the past are inconsistent with the facts and need complete revision. First, however, we complete the picture by examining how they are distributed.

6.2.3 *Distributions*

Up to this point, we have treated cores as if they were isolated objects. They are, however, clustered within clouds, often lying like beads in a chain, within lower density streamers of molecular gas. Clusters and collections of globular-like cores are also found. In this sense, star formation is a regional phenomena. The core clustering in ρ Ophiuchus, displayed in Fig. 6.3, appears to be best describable as fractal.

It has been proposed that the stars we see are pre-determined by the core properties. Specifically, one can envisage that the masses of the stars are equal or proportional to the masses of the cores. We need to be more precise since stars of different mass have vastly different lifetimes. Thus, we compare the distribution in core masses to the rate at which stars of each mass are being created. The latter is quantified by a probability distribution function called the Initial Mass Function (see §12.7).

Mass determinations derived through studies of molecular line emission

have led to reports that the two distributions are not the same. Many large fragments are detected, including unbound features, and so we describe the resulting number distribution as the molecular *clump* spectrum. The observations yield power law distributions mainly in the range

$$\frac{dN_{clump}}{d\log M} \propto M^{-(0.6\pm0.3)}, \tag{6.8}$$

which is essentially the same law as applies to clouds in general (Eq. 3.8): most clumps are small yet most mass is still contained in the largest entities. Note that throughout this book we try to express all distributions in terms which emphasise where most of the number, mass or energy lies. We thus separate any counts into logarithmic bins. The value where the distribution peaks is then a true characteristic measurement (later, we will process photon counts similarly, to present spectral *energy* distributions (SEDs) rather than photon *number* distributions).

Core mass distributions are estimated using submillimetre dust fluxes. Through the dust, one measures the total mass much more accurately. Compact gravitationally bound objects are selected. For ρ Ophiuchus, the distribution of number per unit mass is shown in Fig. 6.3. Perhaps three power-law fits are needed to characterise the distribution. As we shall see, this resembles the number-mass distribution for stars (§12.7). Note that the mean core mass is well below one solar mass and that there are very few high mass cores. These properties are typical of cores in other locations such as Taurus, Orion B and Serpens.

6.3 Classical Collapse Scenarios

Astronomers have been active in seeking the initial conditions for star formation. In the classical collapse picture the fundamental initial assumption is a core at rest but on the verge of collapse. The ideal situation of a uniform sphere is also often taken. The objective is to relate the static core properties to the final stellar properties by calculating the evolution.

It was soon realised that a uniform core would cool and lose thermal support. The collapse consequently becomes dynamic, possibly in gravitational free-fall. Systematic motions reach supersonic speeds. A small protostellar core then forms and residual gas accretes dynamically onto the core.

The full story, however, is not so simple. Besides the many choices of

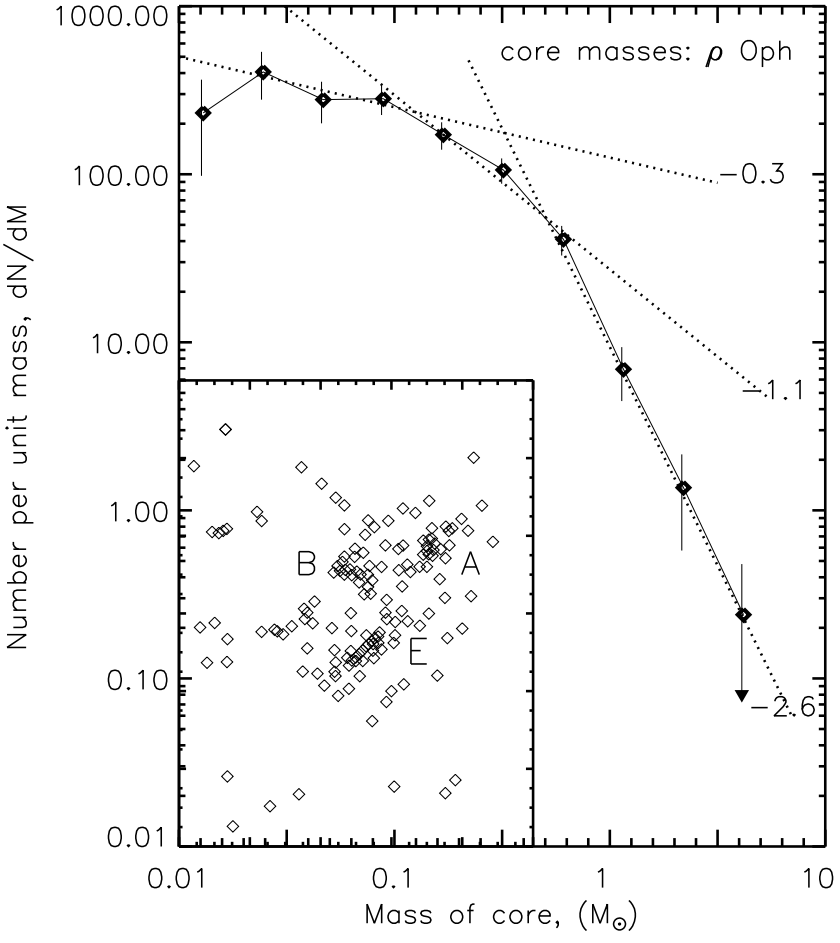

Fig. 6.3 The number distribution by mass of the cores in ρ Ophiuchus for 118 small-scale fragments. The dotted lines show power-law fits of the form $dN/dM \propto M^{\alpha}$. The error bars correspond to $\sqrt{N}$ counting statistics. The inset displays the core positions in a wide region stretching $1^{\circ} \times 1.2^{\circ}$, with the locations of the clumps A, B and E marked (courtesy of T. Stanke, R. Gredel, T. Khanzadyan).

initial conditions (magnetic field, rotation, shape and internal structure), there is a wide range of physics (radiation transport, self-gravity, thermodynamics and chemistry), dynamical mechanisms (magnetic field diffusion, turbulent viscosity, shock wave formation) and external influences (tidal effects, radiation field, shock waves, cloud collisions) to include.

Starless cores are cold and the long wavelength radiation emitted is free to escape. This means that, provided the temperature does remain low, we can treat the cores as isothermal. The temperature may not remain quite constant but it should be a good approximation until the collapse begins to release large amounts of gravitational potential energy. Although cold, thermal pressure remains significant: a pressure-less approximation is not really justified. The approximation, however, has provided insight, demonstrating that the free-fall collapse (in the time given by Eq. 4.1) leads to fragmentation and that the spherical symmetric solution is singular: any small deviation from symmetry will grow and the cloud will flatten.

The collapse of isothermal spheres has provided a strong focus of research. Solutions beginning from a stationary uniform cloud were first tried independently by Larson and Penston in 1969 but they remain too theoretical to exploit. Nevertheless, these solutions demonstrated the tendency towards a collapse at 3.3 times the sound speed. One goal was to find solutions in which the gas smoothly settles onto a central compact object. The initial conditions, however, first lead to a supersonic collapse which can only be abruptly braked.

In what can be considered as the standard view, Frank Shu and others have successfully argued that a singular isothermal sphere can develop with a radial distribution of the form $\rho \propto 1/R^2$. In this scenario, a core may begin in a state just beyond marginal stability, the critical Bonnor-Ebert sphere (§4.3.3). The envelopes of such states possess density profiles close to the form $\rho \propto 1/R^2$ and the central concentration becomes enhanced during an initial slow collapse, producing in theory the singular sphere. An inside-out collapse ensues in which the central region collapses and accretes well before the outer envelope. The central region then undergoes free-fall collapse and the density takes the modified form $\rho \propto 1/R^{3/2}$ and the free-fall speed is $v_{ff} \propto -1/R^{1/2}$ (since $v_{ff}^2 = -GM/R$). The size of the inner region grows as an expansion wave propagates outwards. This theory predicts that the rate at which mass falls onto a central accreting nucleus or 'protostellar core' remains constant in time since the mass inflow rate is $4\pi R^2 \rho v_{ff}$. These predictions allow the model to be tested.

6.4 Core Theory

Many origins for the cores have been proposed. Models which have found support include the following.

- Evolution of clumps through a succession of equilibrium configurations.
- Cold dense clumps in a warm diffuse medium produced through thermal instability.
- Gradual collapse through the extraction of a resisting magnetic field via ambipolar diffusion, as described in §7.5.
- Compression via long-lived non-linear Alfvén waves (§7.2).
- Compression after clump collisions.
- Chance appearance of high density peaks within supersonic turbulence.

In the complex interstellar medium, circumstances where each is responsible are likely to be met. However, we seek the dominant processes which create the majority of stars. In this sense, most models appear to be too restrictive in application.

Fragments not held together by self-gravity are the outcome of many of the above models. There are at least three processes by which a cloud fragment would then grow in mass to become a core. In addition to ambipolar diffusion of neutral material across magnetic field lines, there is Bondi-Hoyle accretion as the clump sweeps through the ambient cloud, or a cooling-driven flow onto the fragment. Other fragments may accumulate mass on a time scale which depends strongly on the mass of the fragment. One would then expect many small cores for each large core. Eventually the large cores would become gravitationally unstable and collapse to form either single or multiple star systems.

Slow infall models appear to have problems fitting the data. The classical hydrodynamic models in which a core evolves rapidly on the inside and gradually on the outside predict that a detectable protostar would be present at the core centre well before the infall regime has become extended, contrary to observations. The collapse in cores such as L1544 seems to proceed in a manner not contemplated by the standard theories of star formation. Our hard work just illustrates how little is still known about the physical conditions that precede birth.

Magnetohydrodynamic models invoke magnetically-supported cores but in which the magnetic field gradually lets the molecules slip through, in the process called ambipolar diffusion (§7.5). Lifetimes of between 3 Myr and 14 Myr are predicted although the critical parameters are not well known. Nevertheless, these lifetimes are an order of magnitude larger than our estimates based on observations.

6.5 Turbulent Evolution of Cores

The suggestion is that our natural tendency to 'begin with' something static immediately puts us on the false track. Since clouds are turbulent at suprathermal speeds, surely we should begin from a dynamic turbulent state? Yet in the observed cores, the turbulence has decayed and clearly does not dominate the pressure. Nevertheless, the 'initial conditions' in the cores are controlled by the state the gas is left in after the decay.

We begin with a turbulent cloud out of which density fluctuations generate fragments, some of which are massive enough to be self-gravitating. These fragments decouple from their turbulent environment, collapsing to protostars with little further external interaction. This mechanism may tend to form low-mass cores. High-mass stars would then require merging of several of these condensations, preferentially occurring in dense highly turbulent gas where collisions would be frequent.

The cores which form out of the turbulence are described as triaxial and distorted, often appearing extremely elongated. Computer simulations show that sheet-like structures form in a medium dominated by supersonic turbulence. The sheets collapse into filaments as self-gravity takes control. The filaments then split up into chains of elongated cores. Also, dense cores develop at locations where filaments intersect. Later in the simulations, as the turbulence dies away, the cores tend to become more regular since the physics becomes dominated by thermal pressure and gravity.

Vital themes not mentioned until now are that of binary formation, cluster formation and the differences between the formations of high and low mass stars. These are themes within which we can compare the objects that we develop against the finished products (see §11.9). Nevertheless, it should be remarked here that we will have to find the means to fragment a core at some stage, and also to form star clusters with diverse properties.

After a long delay, the work on supersonic turbulence is progressing fast and we will soon be able to predict the core structure and evolution in detail. The results will depend on the physical and chemical input into the computer simulations. Therefore, although it is clear that cores are the mediating phase between the cloud and the collapse into stars, we need to take a fresh look at the context in which the physical processes operate. This we do in the next chapter. First, however, it is worthwhile to let the core collapse run its course up to the critical moment.